

# Learning Science Through Research

**Published by the Keck Geology Consortium** 

Short Contributions Keck Geology Consortium Volume 36 May 2024 doi: 10.18277/AKRSG.2024.36.02

# THE ROLE OF FAULT DAMAGE ZONES IN STRUCTURALLY CONTROLLED LANDSCAPE EVOLUTION, SEVIER FAULT ZONE, SOUTHERN UTAH

PIERCE HAYTON, Colorado College

Project Advisors: Tyler Grambling, Sarah Schanz

#### INTRODUCTION

The relationships between fault systems, weathering, and erosion strongly affect how local landscapes evolve. As a fault propagates it creates a damage zone, characterized by intense fracturing in the lithology surrounding the fault. Fault damage zones associated with normal faults can develop asymmetrically, further influencing the regional and local fault geometry, as well as the underlying structural geology. Damage zone asymmetry often presents as both an asymmetry in damage zone width and sometimes as an asymmetry in the fracture distribution and density. The damage zone within hanging walls can be much wider than the within the footwall (Berg and Skar, 2005; Choi et al., 2016), resulting in a much larger volume of rock being affected by fracturing and fracture networks. Damage zones can often be divided into a more intense inner zone and less intense outer zone. Fracture networks and damage zones can sometimes influence fluid flow and drainage patterns, which, in turn, influence weathering and erosion of the highly fractured rock.

This study investigates the relationship between damage zone development and the morphology of fault-controlled landscapes, specifically along the Spencer Bench fault segment of the Sevier Fault. The results shed light on the style of topographic evolution in fault-controlled landscapes. Exploring this phenomenon along an active fault splay will lead to a broader understanding of the linkage between tectonic stress, strain, and physical landscapes.

# **STUDY AREA**

The Sevier Fault is in the transition zone between

the Basin and Range Province and the Colorado Plateau physiographic provinces. The Sevier Fault is a sequence of six separate fault segments that have linked to form an interconnected fault network. The fault network now acts as one large, laterally continuous fault due to the linkages that formed across segments (Taylor et al., 2024). This study focuses on a fault-parallel side drainage into Red Hollow Canyon near Orderville, UT (Figure 1). Within the side drainage, the Spencer Bench fault segment almost exclusively displaces the Navajo Sandstone. The drainage trends NE-SW, parallel to fault strike, and displays approximately 10m of displacement at the northern tip and decreases to about 5m at the southern end. The western slope is comprised of the hanging wall of the fault segment, while the eastern slope consists of the footwall. Despite lithologic consistency across the fault, the slope of the hanging wall is significantly shallower than the slope of the footwall. This drainage exhibits headward, apparently fault-controlled, erosion that has resulted in younger exposures being located at the northeast tip of the canyon and older exposures at the mouth to the southwest. As a result, the northern end has undergone the least erosion while the southern end has experienced the greatest amount of erosion.

#### **METHODS**

#### Field Methods

While in the field, we measured fracture orientation and position along each scanline. We determined strike, dip, and dip direction of fractures using Brunton Compasses and we measured position using a handheld meter tape, which we then collated with

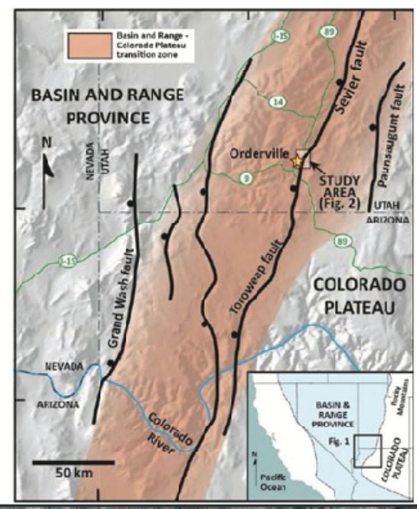




Figure 1. Location of our greater study area, Orderville, UT, and my specific study area. The trace of the Spencer Bench fault segment is highlighted by the dashed, white line in the lower map.

structural data from previous years. We recorded UTM coordinates of start- and end-points of all scanlines using handheld GPS units. We used scanline data to calculate statistics such as fracture intensity. Large portions of the landscape and fault trace were inaccessible by foot, so we used an unmanned aerial vehicle (UAV) to record video of inaccessible outcrops.

#### **3D Structure from Motion (SfM)**

While video of inaccessible outcrops is useful, producing georeferenced 3D models allows for quantitative interpretation of outcrop characteristics. UAV video was imported into Agisoft Metashape Professional to create 3D models by finding overlapping points between captured video frames. Although it is difficult to use SfM models are not high enough resolution to measure fracture orientation, such as strike and dip, it is possible to measure the fracture spacing within these regions. I georeferenced precise locations on each model using coordinates

gathered in Google Earth Pro to ensure that I could measure real-world distances and accurately measure spacing between visible fractures. We then used these data to calculate fracture density.

#### **Cross-Sectional Topographic Profiles**

Due to the drainage exhibiting headward erosion, I constructed seven, down-drainage cross-sectional topographic profiles to compare potential asymmetry in rates of erosion within the hanging wall compared to the footwall. Because the northernmost profiles are the youngest, and the southernmost are the most mature, any asymmetry in erosion rates should become more prevalent moving south the drainage. The northernmost profiles should display the least slope asymmetry, due to having had the least amount of time to erode. These profiles were constructed using ArcGIS Pro and 1m digital elevation models.

## **RESULTS**

#### Fracture Intensity and Spacing

I calculated the average fracture intensity and the damage zone width within the hanging wall and footwall of the Spencer Bench fault segment. This was done from both the data measured in the field and from the 3D SfM models. As shown in Table 1, the damage zone width within the hanging wall is significantly larger (190m) than it is within the footwall (94m). The average fracture spacing, standard deviation, and median of fracture spacing also display this asymmetry; the hanging wall displays a higher fracture intensity than the footwall. The damage zone extends nearly twice as far into the hanging wall than it does into the footwall. Although there is a lack of consensus on how to best define the outer boundary of damage zone (Choi et al., 2016), I defined the outer boundary of the damage zone as the point at which the frequency of deformation becomes equal to the value found further from the fault trace, as described by Choi et al. (2016).

# Down-drainage Cross-sectional Topographic Profiles

I constructed seven cross-sectional profiles in the canyon to assess any asymmetry in slope and the

Table 1. Observed and calculated values for the Spencer Bench fault segment.

	Hanging Wall	Footwall
Damage Zone Width (m)	191.4	94.4
Number of Observations	86	35
Mean Fracture Spacing (m)	1.4	9.1
Fractures per meter	0.71	0.11
Fracture Spacing STDev (m)	2.0	8.0
Fracture Spacing Median (m)	0.7	6.8

effects of fault-driven landscape evolution. Figure 2 shows the location of these profiles, and Figure 3 shows these profiles graphed. These profiles are graphed at their respective elevations and normalized to one datum in order to qualify morphological changes throughout the profiles down drainage. Although the hanging wall slope is visibly shallower than the footwall, there is no discernable pattern in profile slope along strike. The slopes of the hanging wall maintain a consistent shape and do not seem to shallow out as the profiles move south.

Following the construction of these profiles, I averaged them over 25 m and 50 m intervals extending from the fault trace (Figure 4). I chose a 25 m interval to assess the landscape immediately surrounding the fault trace and the 50 m interval to constrain how the landscape evolves over a wider portion of the canyon. I was hesitant to average over the entirety of the profiles because: 1) some of these profiles extend onto adjacent topography and 2) some of these profiles begin to include terrain from the nearby plateau, or extend over a ridge into another canyon. As can be seen in Figure 4, the profiles in the 25 m interval continue to display little to not pattern, but the semblance of a pattern begins to emerge in the 50 m interval. Profiles 1 and 2 seem to decrease in slope difference, with differences of 32° and 15° respectively. Profiles 3 through 7 exhibit a gentle but steady pattern of increase in slope difference. Profile 3 only has a difference in slope of 11° which steadily grows to a difference of 18° by Profile 7.

#### DISCUSSION

#### **Damage Zone Width and Fracture Intensity**

Field data indicate that the damage zones within the hanging wall and footwall are asymmetrical, with a difference in width of nearly 100m. This agrees with previous research from the nearby Moab Fault by Berg and Skar (2005), who found that the damage zone can

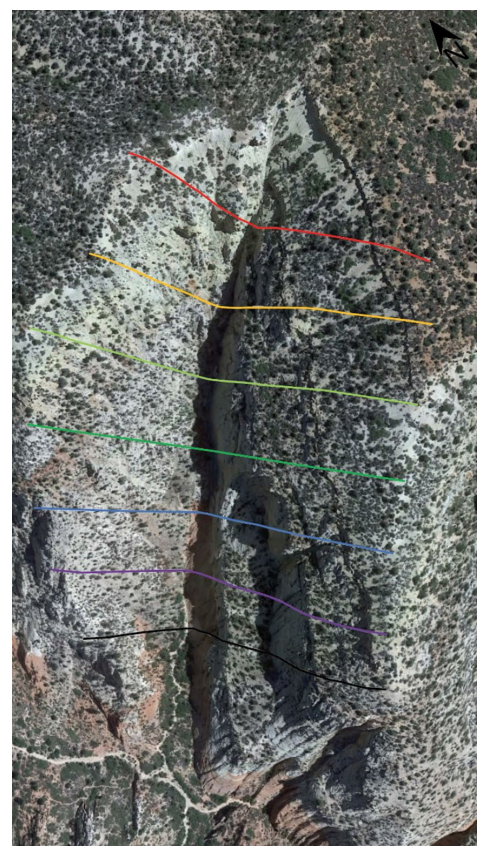
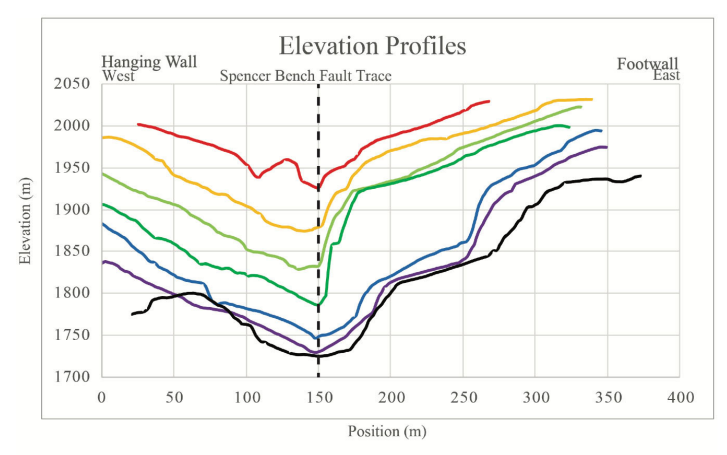


Figure 2. Location of seven cross-sectional down-drainage profiles, each profile is color coded across Figure 3.

be upwards of three times as wide in the hanging wall than it is within the footwall. This asymmetry is also found in fracture intensity data, as the average fracture spacing within the hanging wall is 1.4m compared to 9.1m in the footwall. This difference in fracture density could be attributed to the lack of an inner damage zone. As the name suggests, this is the inner most region of the damage zone, sometimes found within the footwall of a fault. Although Berg and Skar (2005) state that it is possible for these damage zones to form without an inner damage zone, it is possible that one exists. If there is a more intense inner damage zone, it would display a much higher degree deformation, and therefore the fracture intensity within the footwall reported here is not completely accurate.

Berg and Skar (2005) attribute the asymmetric damage zone development to a difference in lithology across the fault. This study provides a new perspective on this problem, as the damage zones studied here are comprised exclusively of the Navajo Sandstone. My findings suggest that damage zone distribution may be affected by something other than lithology. One alternative option for damage zone width control is



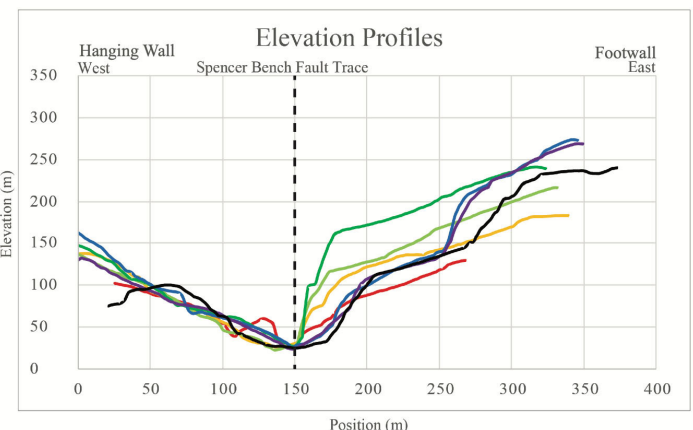


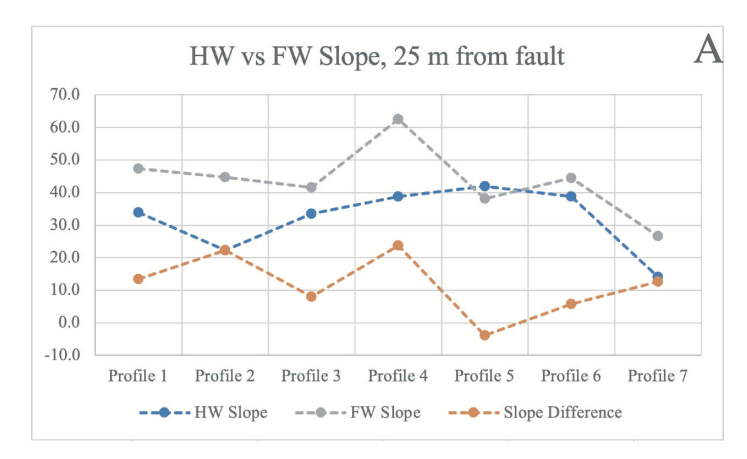
Figure 3. Topographic profiles from Figure 2. The graph on top has these profiles at their respective elevation, while the lower graph has them normalized to one elevation toreveal patterns.

the density of microfractures across the fault blocks. While we did not measure microfracture density at this study site, we do know that microfracture distribution can be asymmetrical (Faulkner et al., 2011). Investigating microfracture density and distribution in the future could help to explain differences seen in slope across the fault trace.

We did not find an inner damage zone within our study area, and while this is not directly at odds with previous research, it is potentially a point of contrast that requires a more detailed assessment of the fault zone than was possible in this work. Regardless, the formation, propagation, and accumulation of displacement along the Spencer Bench fault segment has caused a variable deformation response between the hanging wall and footwall.

#### **Topography Across the Fault**

My initial hypothesis was that the northernmost profiles (red lines in Figs. 3, 4) would display the greatest amount of symmetry between the hanging



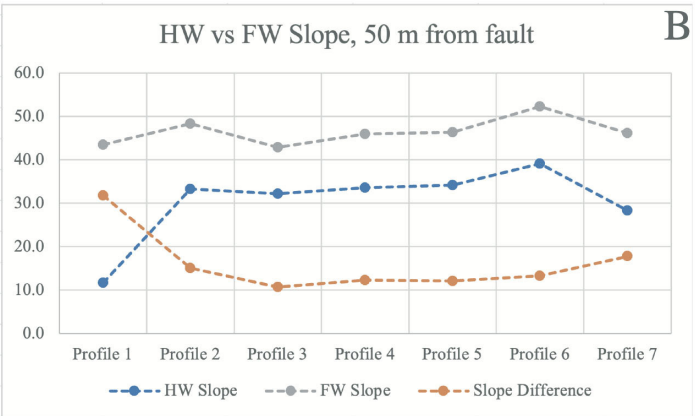


Figure 4. Average slope of the hanging wall, footwall, and difference between the two over A) 25 m interval and B) 50 m interval from the fault trace.

wall and footwall, as fracture-enhanced weathering and erosion would not have had sufficient time to present. As the profiles moved south, I expected the western, hanging wall side of the canyon to shallow out more quickly than the footwall. Thus, the profiles would become more asymmetric as they moved south as exposures increased in age and accumulated strain. As can be seen in the normalized graph in Figure 3, this pattern is not visible, and slope does not have a strong correlation with exposure age across a 25 m swath.

In the 50 m profiles (Figure 4), there is a weak correlation between slope and spatiotemporal distribution along strike, although it is still not as strong as I initially hypothesized. If the northernmost profiles were the most symmetric, then we would expect the slope difference to be close to zero and would increase as the profiles moved south. The difference in slope in the 25 m interval seems to jump around erratically. In the 50 m interval though, Profiles 3 through 7 display a gradual increase in

slope difference from a difference of 11° in Profile 3 to 18° by Profile 7. Profiles 1 and 2 decrease in slope difference, rather than increasing as observed in the southernmost profiles.

The difference in Profiles 1 and 2 may be because Profiles 1 and 2 may extend into the White Throne member of the Temple Cap sandstone in the highest elevations of the canyon. Although this drainage is comprised almost exclusively of the Navajo Sandstone, there are a few meters of the White Throne member at the top of the canyon. We unfortunately do not have a measurement of this member here, but it may be possible that Profiles 1 and 2 extend into this member. If this is the case, the White Throne member may have difference lithologic and physical properties driving erosion to manifest differently in these two profiles. Another potential explanation is that these profiles may be young enough that drainage networks and variations in precipitations have not had sufficient time to normalize like they have in the older, more mature profiles. It is also possible that the adjacent plateau may be close enough to have an effect on rates of erosion. Irregularity of slope difference at a 25 m interval and in the uppermost extent of the canyon may indicate that there is a threshold length and rate at which enhanced fault damage zone erosion correlates with topographic response.

## **CONCLUSIONS**

This drainage into Red Hollow Canyon is an excellent location to study the relationships between fracture intensity and landscape evolution. The studied portion of the Spencer Bench fault segment allows us to isolate the role of landscape response to faulting, as lithology and climate are consistent across the fault trace. Understanding how underlying structures can influence local or regional landscape evolution is key to mitigating secondary, fault-related hazards and provide better understanding of the relationship between fracturing and landscape evolution. This is especially important as land use in structurally controlled regions becomes more prevalent.

Throughout this section of the Spencer Bench segment, the damage zone is asymmetric across the fault. This is in line with previous research on normal faults in the transition zone between the Basin and Range and Colorado Plateau physiographic provinces (Berg and Skar, 2005). The fracture networks are also more intense within the hanging wall than within the footwall. This points towards a greater partitioning of strain into the hanging wall than the footwall. These findings are in line with previous research describing damage zone asymmetry. Furthermore, these findings indicate that such asymmetry is not controlled by a lithologic contrast and may result from the distribution of stress across fault zones.

While the damage zone and fracture network are asymmetrical there is a spatiotemporal dependence to this asymmetry. There is little to no pattern in slopes between the hanging wall and footwall along the 25 m profile lines. The slopes vary greatly from one profile to the next, with no clear trend, which may be due to the interval being too small to draw meaningful conclusions from. A pattern does emerge in the 50 m interval in Profiles 3 through 7. This pattern of gentle increase in slope difference as the profiles move south was my initial hypothesis. The slope difference increases from 11° in Profile 3 to 18° in Profile 7. Profiles 1 and 2 do not follow this pattern, potentially due to the duration of surface exposure or a lithologic contrast in the distal portions of the canyon.

Following these results, there is a weak correlation between underlying geological structures and landscape evolution. Berg and Skar (2005) attribute damage zone asymmetry to a lithology asymmetry across a fault. This study presents evidence that damage zones are asymmetric within normal fault systems even when lithology is consistent. Within this singular lithology, erosion rates have been accelerated within the hanging wall compared to the footwall. We also found an asymmetry in damage zone intensity and distribution; they extend ~100 m further and present more intensely in the hanging wall than the footwall. While further study is needed to explore mechanisms dictating this behavior, it is apparent that asymmetric damage zones are typical of upper crustal normal faults.

# **ACKNOWLEDGEMENTS**

This material is based upon work supported by the

Keck Geology Consortium and the National Science Foundation under Grant No. 2050697. Funding was also provided by NSF Award No. 2042114 to PI Benjamin Surpless. Special thanks to Dr. Ben Surpless for leading this project, and to my advisors Dr. Tyler Grambling and Dr. Sarah Schanz.

## **REFERENCES**

- Berg, S., and Skar, T., 2005, Controls on damage zone asymmetry of a normal fault zone: oyutcrop analysises of a segment of the Moab Fault, SE Utah: Journal of Structural Geology, v. 27, p. 1803–1822, doi:https://doi.org/10.1016/j.jsg.2005.04.012.
- Choi, J.-H., Edwards, P., Ko, K., and Kim, Y.-S., 2016, Definition and classification of fault damage zones: a reivew and a new methodological approach: Earth-Science Reviews, v. 152, p. 70–87, doi:https://doi.org/10.1016/j.earscirev.2015.11.006.
- Faulkner, D.R., Mitchell, T.M., Jensen, E., and Cembrano, J., 2011, Scaling of fault damage zones with displacement and the implications for fault growth processes: Journal of Geophysical Research, v. 116, p. B05403, doi:10.1029/2010JB007788.
- Taylor, W.J., Surpless, B., and Schiefelbein Kerscher, I.M., 2024, Complex Segment Linkage Along the Sevier Normal Fault, Southwestern Utah: Lithosphere, v. 2024, doi:10.2113/2024/lithosphere\_2023\_332.